THE JOURNAL OF PHYSICAL CHEMISTRY Letters

LETTER

pubs.acs.org/JPCL

Direct-Coupling O_2 Bond Forming a Pathway in Cobalt Oxide Water Oxidation Catalysts

Lee-Ping Wang and Troy Van Voorhis*

Department of Chemistry, Massachusetts Institute of Technology, 77 Massachusetts Avenue, Cambridge, Massachusetts 02139, United States

Supporting Information

ABSTRACT: We report a catalytic mechanism for water oxidation in a cobalt oxide cubane model compound, in which the crucial O−O bond formation step takes place by direct coupling between two $Co^{IV}(O)$ metal oxo groups. Our results are based upon density functional theory (DFT) calculations and are consistent with experimental studies of the CoPi water oxidation catalyst. The computation of energetics and barriers for the steps leading up to and including the O−O bond formation uses an explicit solvent model within a hybrid quantum mechanics/molecular mechanics (QM/MM) framework, and captures the essential hydrogen-bonding effects and dynamical flexibility of this system.

SECTION: Energy Conversion and Storage

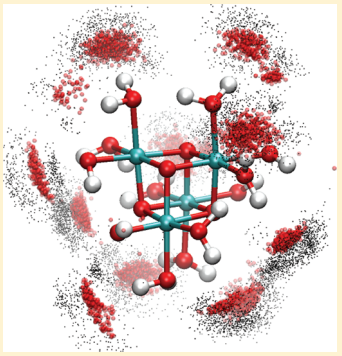

Metal oxides play a central role in the water oxidation half-reaction (also known as the oxygen evolution reaction), an essential and mechanistically complex component of electrochemical water splitting. Metal oxide motifs can be found in a wide range of water oxidation catalysts, ranging from solid-state materials[1,2] to molecular catalysts containing metal−oxo clusters[3,4] and oxo-bridged metal dimers.[5,6] More recently, a cobalt phosphate water oxidation catalyst[7−11] (CoPi) has generated particular interest due to its ease of synthesis, high activity at neutral pH, and robustness in a wide range of operating environments,[12−14] but the structure and mechanism of catalysis are presently unclear.

Here we report a theoretical investigation of the water oxidation mechanism in a cobalt oxide cubane model compound based on CoPi. We find a direct coupling pathway between two $Co^{IV}(O)$ oxo groups across a cube face (Figure 1, outer ring) as a possible operative mechanism for O−O bonding. The proposed mechanism falls within the guidelines delineated by experimental studies.[15] A distinguishing charateristic of this mechanism is the occurrence of O−O bonding after only two out of four oxidation events in the overall cycle, avoiding the energetically costly buildup of four Co^{IV} redox equivalents. Our results are based upon a careful screening of many possible mechanisms and verified by hybrid quantum mechanics/molecular mechanics (QM/MM) calculations of standard reduction potentials ($E°$) and free energy barriers. This study serves as a helpful guide to future studies of the water oxidation mechanism in metal oxide-containing systems and contributes to the knowledge base for rational electrocatalyst design.

Model Catalyst. The model catalyst **1**, shown in Figure 1, contains four octahedrally coordinated Co^{III} atoms (in teal) in a Co_4O_4 cubane core. Each Co atom is additionally coordinated to one hydroxo (OH) ligand and two aqua (OH_2) ligands. The compound is electrically neutral. The geometry-optimized structure of **1** gives Co−O distances and Co−Co distances in good agreement with Fourier-transformed X-ray absorption spectroscopy (XAS) data on CoPi at short distances (Figure S1, Supporting Information).[16,17] Our model does not contain phosphate ligands, as the XAS interpretation does not suggest a structural role for phosphate. This is supported by the experimental finding that the catalytic activity is preserved when phosphate is replaced with structurally distinct buffering electrolytes such as methyl phosphonate.[9,18]

Our choice of using a minimal functional model with the basic chemical features of CoPi follows a principle of parsimony; the results based on the model are applicable to the experimental system, as long as a percentage of the amorphous material contains the chemically active motifs.[15] The single cubane model is smaller and simpler than the corner-sharing cubane[16] and molecular cobaltate cluster[17] models of CoPi proposed in the XAS studies, which were designed to agree with structural details at interatomic distances greater than 3 Å. We note that updating the model compound with structural details would likely contribute to a more exhaustive description while keeping this mechanistic proposal qualitatively intact. Our model also shares similarities with proposed oxygen-evolving complex (OEC) structures[19] and other water oxidation catalysts with metal−oxo cores,[3,4] which makes this study helpful for understanding a wide scope of systems.

Received: July 27, 2011
Accepted: August 17, 2011
Published: August 17, 2011

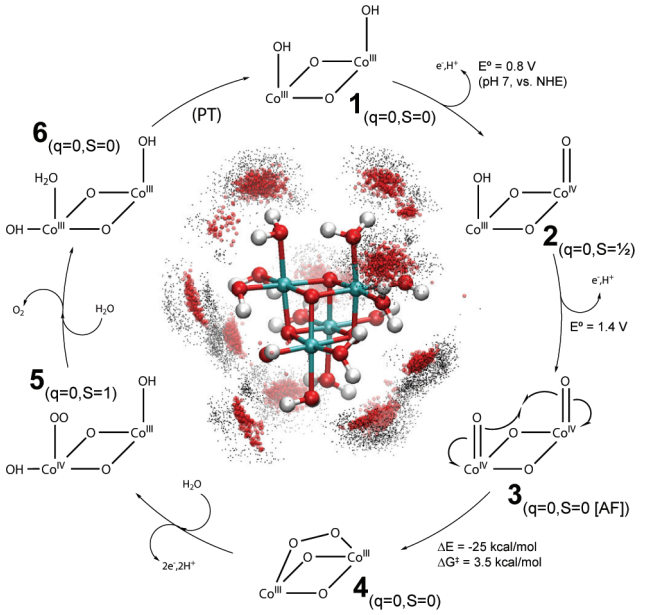

Figure 1. Outer ring: Proposed mechanism of water oxidation catalysis; intermediates are labeled in bold face, with net charge and lowest-energy spin state in subscript (AF denotes an open-shell electronic state with antiferromagnetic coupling). Standard reduction potentials ($E°$) and free energy barriers for the first half of the cycle, computed by QM/MM, are given. Terminal aqua ligands and the bottom half of the compound are omitted for clarity. Center: MM dynamics trajectory of model catalyst structure (held static) with superimposed positions of nearby explicit solvent water molecules (oxygen: red spheres; hydrogen: black dots), highlighting the strong hydrogen-bonding effects.

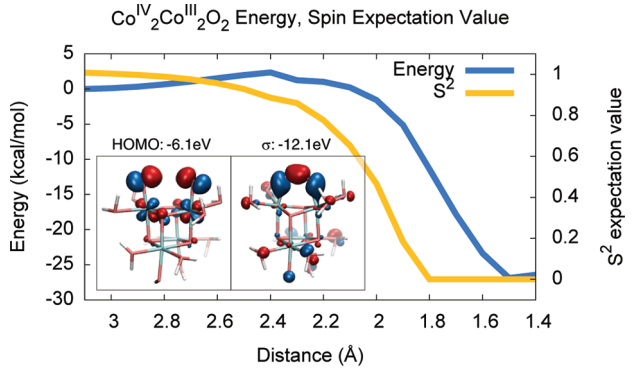

Figure 2. DFT energies (left *Y*-axis, in blue) and $\langle S^2 \rangle$ (right *Y*-axis, in orange) as a function of O−O distance for the doubly oxidized model catalyst, **3**. Left inset: highest occupied molecular orbital (HOMO) at r_{OO}= 3.0 Å. Right inset: σ bonding orbital at r_{OO} = 1.4 Å.

Mechanistic Exploration. We searched the configuration space of the singly and doubly oxidized compound for stable O−O bonded structures. The energies of all relevant structures were computed using density functional theory (DFT); oxidation events, which are experimentally shown to be proton-coupled, were represented by removing hydrogen atoms from **1** . Among the many structures we examined, we found that a doubly oxidized compound with two cofacial $Co^{IV}(O)$ oxo groups formed a stable O−O single bond with a very low activation barrier (**3** → **4**).

We found that O−O bonding along this coordinate has a reaction energy of −27.3 kcal/mol with an activation energy of

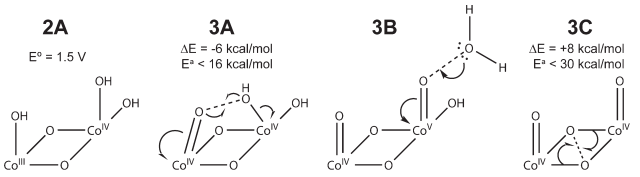

Figure 3. Energetically disfavored structures and pathways. **2A**: An alternative protonation state of **2**, containing a Co^{IV} bis-hydroxo; $E°$ (labeled) is significantly higher than that of the **1**/**2** couple. **3A**, **3B**, **3C**: Alternative O−O bonding pathways with reaction energies and activation barriers labeled; the computations for **3B** included extra water molecules or phosphate anions as proton acceptors (not shown). **3B** was ruled out because Co^{V} was a prerequisite to reactivity.

2.3 kcal/mol (Figure 2). The value of $\langle S^2 \rangle$ for the ground state wave function went from 1.0 (broken symmetry) to 0.0 (closed shell), indicating the formation of a single bond from two radicals. The two unpaired electrons in **3** are antiferromagnetically coupled in the ground state, as the ferromagnetically coupled triplet state is 1.6 kcal/mol higher in energy. The singlet diradical state also appears necessary for bond formation as the O−O interaction is repulsive in the triplet state.

The oxo groups have strong radical character, similar to the Baik group's results for the blue dimer[20] but involving different *d* orbitals.[21] A spin density plot is given in Figure S4 (Supporting Information), suggesting that these $Co^{IV}(O)$ groups are formally closer to being $Co^{III}(O\bullet)$ radicals; however, we shall retain the $Co^{IV}(O)$ notation for simplicity. Molecular orbital analysis of **3** and **4** (Figure 2 insets and Figure S2, Supporting Information) shows the formation of a σ bond along with doubly occupied π bonding and π^* antibonding orbitals for a total bond order of 1.

Our investigation touched on many other O−O bonding pathways, which were all rejected based on unfavorable energetics. An O−O bond between $Co^{IV}(O)$ and $Co^{IV}(OH)$ groups was found (Figure 3, **3A**), but the barrier was much higher compared to coupling between two $Co^{IV}(O)$ groups. Nucleophilic attack of a solvent water molecule on a terminal oxo (i.e., acid−base mechanism, **3B**) was observed only if at least one cobalt atom was oxidized to $Co^{V}(O)$; this was ruled out for lack of experimental evidence for Co^{V}. Earlier studies on ruthenium complexes indicate that the acid−base mechanism requires a $Ru^{V}(O)$ intermediate,[22,23] similar to our requirement for Co^{V} here. No O−O bonding occurred between a solvent water molecule and any $Co^{IV}(O)$ group, even when up to three additional water molecules or phosphate groups were included in the calculation as hydrogen bond/proton acceptors. Some O−O bonded structures were found involving μ-oxos in the cubane core (**3C**), but the activation barriers for liberating the resulting O_2 molecule proved too great, as it required breaking many Co−O bonds.

Following the investigation of O−O bonding, we explored the subsequent O_2 liberation step. The addition of one water molecule directly to **4** can lead to displacement of the bridging O−O group coupled with intramolecular proton transfer (PT), resulting in terminal OOH and OH groups. This process was found to be downhill but with a very high barrier (ΔE = −12.9 kcal/mol, E^a < 35 kcal/mol), as the transition state involves the breaking of an O−H bond and a Co−O bond. This imposing barrier was significantly lowered if the third and/or fourth proton-coupled oxidation events in the overall cycle were allowed to occur prior to water addition. When the water addition reaction was examined for

Table 1. Standard Reduction Potentials (E°) Computed by QM/MM

reduced	oxidized	E° (vs NHE, pH 7)
1	**2**	0.8 V
1	**2A**	1.5 V
2	**3**	1.4 V

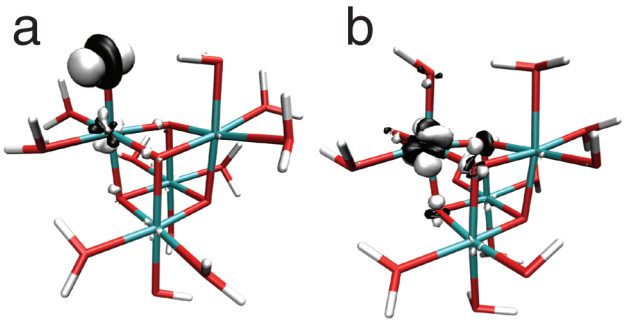

Figure 4. Plots of the hole density for two isomers of the once-oxidized complex. (a) The terminal oxo species **2**. The hole density resembles an antibonding orbital and indicates that an oxidation event contributes to increased bond order. (b) The bis-hydroxo species **2A**, showing localization of the hole on the cobalt atom.

the once-oxidized (twice-oxidized) equivalents of **4**, we found that the energetics were $\Delta E = -9.3$ kcal/mol, $E^a = 6.8$ kcal/mol ($\Delta E = -8.3$ kcal/mol, $E^a < 9$ kcal/mol); the barrier height was significantly reduced. These results suggest that at least one proton-coupled oxidation of **4** occurs before water addition.

Adding water to the once-oxidized or twice-oxidized equivalents of **4** displaces the bridging O−O group without transferring a proton, resulting in terminal OO and OH_2 ligands; the combination of two oxidations and water addition thus leads to **5**. Adding a second water to **5** releases molecular dioxygen ($\Delta E = -13.4$ kcal/mol, $E^a = 4.0$ kcal/mol), leading to **6** which is simply an isomer of **1**; the catalytic cycle is then closed by intramolecular PT.

QM/MM Computation of Free Energies. For O−O bonding to take place via the proposed cycle in Figure 1, the steps must be thermodynamically and kinetically viable, especially in comparison to alternative pathways. Thus, it is vital to accurately compute E° for the various oxidation steps and free energy barriers for the chemical steps. We found that an explicit solvent model was essential for this task, as it accounts for hydrogen bonding effects which are not present in gas-phase DFT or implicit solvent models. This is highlighted by results from exploratory classical simulations in which we found strong hydrogen bonding effects (Figure 1, center). The solute was also likely to be highly flexible (Figure S3, Supporting Information), suggesting that configurational averaging might be necessary to accurately evaluate E° . For these computations we used a QM/MM simulation framework, where the solute is treated using DFT and the solvent is treated using a polarizable classical model; the underlying theory and details of the simulation method are given in the Supporting Information.

We computed the first two E° values in explicit solvent (Table 1). The protonation state of the oxidized species had a major effect on the E° value for the first oxidation event. When the oxidized species contained a $Co^{IV}(O)$ group (**1**/**2**; first row), the E° value was 0.7 V lower compared to the alternative pathway

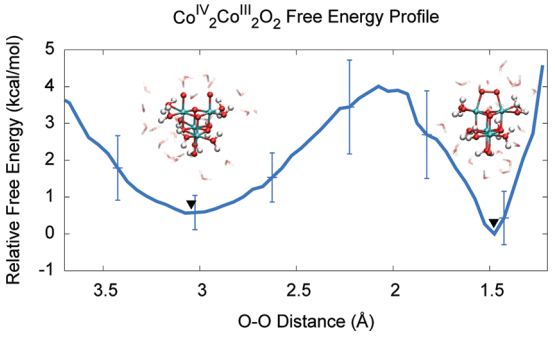

Figure 5. QM/MM free energy profile as a function of O−O distance for the direct coupling pathway (**3** → **4**). Simulation snapshots are shown for the free energy minima at r_{OO} = 3.0 Å and r_{OO} = 1.4 Å, indicated by triangles. Error bars were derived from the statistical uncertainty of the probability distribution over the ensemble of QM/MM simulations.

leading to two $Co^{IV}(OH)$ groups (**1**/**2A**; second row). This indicates that an terminal oxo is an energetically favorable protonation state and increases the probability for participation of terminal $Co^{IV}(O)$ groups in the mechanism.

The low redox potential associated with forming $Co^{IV}(O)$ (**2**) relative to a second $Co^{IV}(OH)$ (**2A**) is an interesting result that deserves some chemical interpretation. This difference in redox potentials can be visually explained by plotting difference densities for electron attachment to these two isomers (Figure 4); this provides a visualization of the hole that is created by the oxidation event. Notably, we found that the hole density on **2** is mostly localized on the terminal oxo group with some population on the cobalt (Figure 4a), and contains a nodal plane bisecting the Co−O bond. This indicates that the electron is removed from a Co−O antibonding orbital, leading to an increase in the bond order and lowering the free energy of the oxidized state. In **2A**, on the other hand, the hole is almost entirely localized on the cobalt atom (Figure 4b), indicating that the oxidation does not cause any change in the bond order. This is in part due to the orientation of the O−H bond on the $Co^{IV}(OH)$ groups, which are controlled mainly by hydrogen bonding effects and interferes with Co−O π-type interactions.

From **2**, a second oxidation event leads to **3** and subsequent O−O coupling. We investigated the free energy barrier to O−O bond formation using the QM/MM dynamics simulations of **3**. Figure 5 is a free energy profile constructed from the probability distribution of O−O distances. Two free energy minima are visible, corresponding to the open and bonded configurations (**3** and **4**); the barrier to bond formation is quite small at ~3.5 kcal/mol, only slightly higher than the barrier calculated using gas-phase DFT. Direct coupling occurred spontaneously (within 2−5 ps) in 14 out of 30 dynamics trajectories, demonstrating that O−O bonding is a fairly rapid step. It should be noted that the true free energy minimum of **4** is likely much deeper than that shown in Figure 5, but an accurate evaluation of the relative well depths would require much longer QM/MM simulations containing multiple bond forming/breaking events.

In summary, we examined the water oxidation mechanism of a cobalt oxide cubane model compound based on the CoPi catalyst. The distinguishing features of the proposed mechanism are

- Two adjacent $Co^{III}(OH)$ moieties are oxidized to $Co^{IV}(O)$ via proton-coupled oxidation events. The $Co^{IV}(O)$ protonation state is significantly favored over $Co^{IV}(OH)_2$, and two

adjacent $Co^{IV}(O)$ groups can be formed at experimentally applied potentials.
- After forming two adjacent $Co^{IV}(O)$ groups, direct coupling occurs to form an O−O bond with a low kinetic barrier and a strong thermodynamic driving force (**3** → **4**).
- The third and fourth proton-coupled oxidation events greatly lower the barrier for adding two water molecules and displacing one O_2 molecule, affording a pathway for catalytic turnover.

The mechanistic proposal reported here can be compared to the mechanism for the two-center Ru-Hbpp catalyst from the Llobet group;[24] a key difference between our results and those of ref 24 is that direct coupling occurs after only *two* out of four oxidations in the present study, whereas direct coupling in Ru-Hbpp requires all four oxidations. The early occurrence of O−O bonding in the cycle may help to lower the overpotential by formally reducing the cobalt centers and avoiding the energetically costly buildup of Co^{IV} redox equivalents. Furthermore, we propose that the third and fourth oxidation events will greatly facilitate subsequent steps involving O_2 release, which have presented significant activation barriers in previous computational studies.[25]

The implications of our study in the context of ongoing experimental investigation are as follows. Recent electrochemical studies have shown that at catalytic conditions there exists a one-electron, one-proton redox couple in minor equilibrium followed immediately by a rate-determining *chemical* step; the identity of this step has been proposed to be O−O bond formation.[15] We found a very low barrier for O−O bonding in our study, suggesting that the identity of the rate-determining step may be something else (for example, addition of a water molecule or intramolecular PT). This result serves as a helpful guide to future mechanistic studies focusing on the identity of the rate-determining step.

We note that the proposed mechanism does not provide a pathway for the extrusion of oxygen atoms from the metal oxide core of the catalyst as suggested by isotope labeling studies.[15] The experimental studies acknowledge that multiple pathways are possible, and the isotope labeling studies may indicate a separate mechanism involving two-coordinate μ-hydroxo moieties that are not present in the current model but suggested in other structures.[17] The mechanism proposed here can be tested against alternative proposals using updated model structures containing new chemical motifs; this is a topic of ongoing work.

Our work represents a significant step toward understanding the catalytic mechanism of this interesting system; while the direct coupling pathway found here is by no means exclusive, the clarity of our theoretical findings suggests that this pathway deserves further experimental investigation. We also plan to apply the QM/MM methodology to compute the third and fourth E° values as well as free energy barriers for water addition and oxygen displacement, providing quantitative verification of the entire cycle.

■ ASSOCIATED CONTENT

Supporting Information. Methodology for DFT and QM/MM simulations, geometry of model catalyst, orbital diagram for O−O bond formation, MM-derived figure showing conformational flexibility of catalyst and explicit solvent, spin density plot of **3**, and XYZ coordinates of intermediates and transition states. This material is available free of charge via the Internet at http://pubs.acs.org.

■ AUTHOR INFORMATION

Corresponding Author
*E-mail: tvan@mit.edu.

■ ACKNOWLEDGMENT

This work was funded by ENI SpA as part of the Solar Frontiers Research Program. L.P.W. thanks Yogesh Surendranath and Dan Nocera for many insightful discussions.

■ REFERENCES

(1) Kiwi, J.; Gratzel, M. Oxygen Evolution from Water via Redox Catalysis. *Angew. Chem., Int. Ed.* **1978**, *17*, 860–861.
(2) Kiwi, J.; Gratzel, M. Ruthenium Oxide, A Suitable Redox Catalyst to Mediate Oxygen Production from Water. *Chimia* **1979**, *33*, 289–291.
(3) Brimblecombe, R.; Swiegers, G. F.; Dismukes, G. C.; Spiccia, L. Sustained Water Oxidation Photocatalysis by a Bioinspired Manganese Cluster. *Angew. Chem., Int. Ed.* **2008**, *47*, 7335–7338.
(4) Yin, Q. S.; Tan, J. M.; Besson, C.; Geletii, Y. V.; Musaev, D. G.; Kuznetsov, A. E.; Luo, Z.; Hardcastle, K. I.; Hill, C. L. A Fast Soluble Carbon-Free Molecular Water Oxidation Catalyst Based on Abundant Metals. *Science* **2010**, *328*, 342–345.
(5) Gilbert, J. A.; Eggleston, D. S.; Murphy, W. R.; Geselowitz, D. A.; Gersten, S. W.; Hodgson, D. J.; Meyer, T. J. Structure and Redox Properties of the Water-Oxidation Catalyst $[(bpy)_2(OH_2)RuORu(OH_2)(bpy)_2]^{4+}$. *J. Am. Chem. Soc.* **1985**, *107*, 3855–3864.
(6) Limburg, J.; Vrettos, J. S.; Liable-Sands, L. M.; Rheingold, A. L.; Crabtree, R. H.; Brudvig, G. W. A Functional Model for O−O Bond Formation by the O_2-Evolving Complex in Photosystem II. *Science* **1999**, *283*, 1524–1527.
(7) Kanan, M. W.; Nocera, D. G. In Situ Formation of an Oxygen-Evolving Catalyst in Neutral Water Containing Phosphate and Co^{2+}. *Science* **2008**, *321*, 1072–1075.
(8) Kanan, M. W.; Surendranath, Y.; Nocera, D. G. Cobalt−Phosphate Oxygen-Evolving Compound. *Chem. Soc. Rev.* **2009**, *38*, 109–114.
(9) Surendranath, Y.; Dinca, M.; Nocera, D. G. Electrolyte-Dependent Electrosynthesis and Activity of Cobalt-Based Water Oxidation Catalysts. *J. Am. Chem. Soc.* **2009**, *131*, 2615–2620.
(10) Lutterman, D. A.; Surendranath, Y.; Nocera, D. G. A Self-Healing Oxygen-Evolving Catalyst. *J. Am. Chem. Soc.* **2009**, *131*, 3838–+.
(11) McAlpin, J. G.; Surendranath, Y.; Dinca, M.; Stich, T. A.; Stoian, S. A.; Casey, W. H.; Nocera, D. G.; Britt, R. D. EPR Evidence for Co(IV) Species Produced During Water Oxidation at Neutral pH. *J. Am. Chem. Soc.* **2010**, *132*, 6882–+.
(12) Jiao, F.; Frei, H. Nanostructured Cobalt Oxide Clusters in Mesoporous Silica as Efficient Oxygen-Evolving Catalysts. *Angew. Chem., Int. Ed.* **2009**, *48*, 1841–1844.
(13) Zhong, D. K.; Gamelin, D. R. Photoelectrochemical Water Oxidation by Cobalt Catalyst ("Co−Pi")/α-Fe_2O_3 Composite Photoanodes: Oxygen Evolution and Resolution of a Kinetic Bottleneck. *J. Am. Chem. Soc.* **2010**, *132*, 4202–4207.
(14) Steinmiller, E. M. P.; Choi, K. S. Photochemical Deposition of Cobalt-Based Oxygen Evolving Catalyst on a Semiconductor Photoanode for Solar Oxygen Production. *Proc. Natl. Acad. Sci. U.S.A.* **2009**, *106*, 20633–20636.
(15) Surendranath, Y.; Kanan, M. W.; Nocera, D. G. Mechanistic Studies of the Oxygen Evolution Reaction by a Cobalt−Phosphate Catalyst at Neutral pH. *J. Am. Chem. Soc.* **2010**, *132*, 16501–16509.
(16) Risch, M.; Khare, V.; Zaharieva, I.; Gerencser, L.; Chernev, P.; Dau, H. Cobalt−Oxo Core of a Water-Oxidizing Catalyst Film. *J. Am. Chem. Soc.* **2009**, *131*, 6936–6937.

(17) Kanan, M. W.; Yano, J.; Surendranath, Y.; Dinca, M.; Yachandra, V. K.; Nocera, D. G. Structure and Valency of a Cobalt−Phosphate Water Oxidation Catalyst Determined by in Situ X-ray Spectroscopy. *J. Am. Chem. Soc.* **2010**, *132*, 13692–13701.

(18) Dinca, M.; Surendranath, Y.; Nocera, D. G. Nickel-Borate Oxygen-Evolving Catalyst That Functions under Benign Conditions. *Proc. Natl. Acad. Sci. U.S.A.* **2010**, *107*, 10337–10341.

(19) Ferreira, K. N.; Iverson, T. M.; Maghlaoui, K.; Barber, J.; Iwata, S. Architecture of the Photosynthetic Oxygen-Evolving Center. *Science* **2004**, *303*, 1831–1838.

(20) Yang, X.; Baik, M. H. *cis,cis*-$[(bpy)_2Ru^{V}O]_2O^{4+}$ Catalyzes Water Oxidation Formally via *in Situ* Generation of Radicaloid $Ru^{IV}-O\bullet$. *J. Am. Chem. Soc.* **2006**, *128*, 7476–7485.

(21) Batista, E. R.; Martin, R. L. Electron Localization in the Ground State of the Ruthenium Blue Dimer. *J. Am. Chem. Soc.* **2007**, *129*, 7224–+.

(22) Concepcion, J. J.; Jurss, J. W.; Templeton, J. L.; Meyer, T. J. One Site is Enough. Catalytic Water Oxidation by $[Ru(tpy)(bpm)(OH_2)]^{2+}$ and $[Ru(tpy)(bpz)(OH_2)]^{2+}$. *J. Am. Chem. Soc.* **2008**, *130*, 16462–16463.

(23) Wang, L. P.; Wu, Q.; Voorhis, T. V. Acid-Base Mechanism for Ruthenium Water Oxidation Catalysts. *Inorg. Chem.* **2010**, *49*, 4543–4553.

(24) Bozoglian, F.; Romain, S.; Ertem, M. Z.; Todorova, T. K.; Sens, C.; Mola, J.; Rodriguez, M.; Romero, I.; Benet-Buchholz, J.; Fontrodona, X.; et al. The Ru-Hbpp Water Oxidation Catalyst. *J. Am. Chem. Soc.* **2009**, *131*, 15176–15187.

(25) Yang, X. F.; Baik, M. H. The Mechanism of Water Oxidation Catalysis Promoted by $[tpyRu(IV)=O]_2L^{3+}$: A Computational Study. *J. Am. Chem. Soc.* **2008**, *130*, 16231–16240.